Nucleation and growth of GaN/AlN quantum dots

C. Adelmann* and B. Daudin
CEA/CNRS Research Group "Nanophysique et Semiconducteurs," Département de Recherche Fondamentale sur la Matière Condensée, CEA/Grenoble, 17 Rue des Martyrs, 38054 Grenoble Cedex 9, France

R. A. Oliver† and G. A. D. Briggs
Department of Materials, University of Oxford, Parks Road, Oxford OX1 3PH, United Kingdom

R. E. Rudd
Lawrence Livermore National Laboratory, 7000 East Avenue, Livermore, California 94550, USA
(Received 21 October 2003; revised manuscript received 8 June 2004; published 29 September 2004)

We study the nucleation of GaN islands grown by plasma-assisted molecular-beam epitaxy on AlN(0001) in a Stranski-Krastanov mode. In particular, we assess the variation of their height and density as a function of GaN coverage. We show that the GaN growth passes four stages: (i) initially, the growth is layer by layer, (ii) subsequently, two-dimensional precursor islands form, which (iii) transform into genuine three-dimensional islands. Island height and density increase with GaN coverage until the density saturates. (iv) During further GaN growth, the density remains constant and a bimodal height distribution appears. A fit of an equilibrium model for Stranski-Krastanov growth to the variation of island distributions as a function of coverage is discussed.

DOI: 10.1103/PhysRevB.70.125427 PACS number(s): 81.07.Ta, 68.37.Ps, 81.10.Aj, 68.55.Ac

I. INTRODUCTION

Zero-dimensional semiconductor quantum dots (QDs) have attracted much interest in the last decade due to their multiple potential applications ranging from low-threshold lasers[1,2] via single-electron tunneling devices[3,4] to possible realizations of qubits for quantum computation.[5,6] A versatile method for the fabrication of semiconductor QDs is their self-assembled growth following the Stranski-Krastanov (SK) growth mode.[7] This mode usually occurs during the growth of semiconductor epilayers under compressive strain. Example material systems are $In_xGa_{1-x}As/GaAs$,[8–10] Si_xGe_{1-x}/Si,[11,12] CdSe/ZnSe,[13] or GaN/AlN.[14–18] In this mode, atoms are initially deposited in form of a two-dimensional pseudomorphic wetting layer. The associated strain energy increases with the thickness of the wetting layer and is finally elastically relieved by the formation of islands.

The usefulness of such self-assembled nanostructures relies on the ability to obtain homogeneous size distributions as well as to control their size, density and position. Many theoretical contributions have enhanced our understanding of the size distributions of SK-grown islands, but some controversy remains.[19–25] Also, despite many experimental studies, the influence of growth parameters on the size and density of such islands is not fully understood, owing to the complexity of the physics of strained layer growth.

In this work, we present results on the nucleation of GaN islands on AlN following an SK mode, in particular on the dependence on the amount of deposited GaN and the substrate temperature. The qualitative behavior is similar to that found in other systems such as, e.g., InAs/GaAs or Ge/Si. This reinforces the idea that there are common features of semiconductor SK growth, which are rather universal and independent of the specific material system. Absolute island sizes and densities will depend on the material system, possibly through material parameters like lattice misfit, elastic constants, or surface energies. Hence, we may further discuss the experimental data in the framework of an equilibrium model based on statistical physics that was originally developed in work on the Ge/Si system.[26]

II. EXPERIMENTAL

The samples have been grown in a MECA2000 molecular-beam epitaxy (MBE) chamber equipped with standard effusion cells for Ga and Al evaporation. The chamber also contains an rf plasma cell to provide active nitrogen for GaN and AlN growth. The pseudosubstrates used were about 2 μm thick GaN(0001) (Ga-polarity) layers grown by metal-organic chemical vapor deposition on sapphire. The substrate temperature T_S was measured by a thermocouple in mechanical contact to the backside of the molybdenum sample holder. To ensure substrate temperature reproducibility, each series of samples described below was grown on a single molybdenum substrate holder.

Prior to all experiments, a 100 nm thick GaN layer was grown under Ga-rich conditions on the pseudosubstrates to avoid the influence of a possible surface contamination layer. Subsequently, a 300 nm thick AlN film was deposited under Al-rich conditions at a substrate temperature of 730 °C. We have found by reflection high-energy electron diffraction (RHEED) and high-resolution x-ray diffraction that this thickness is sufficient for the AlN layer to be virtually fully relaxed with a residual in-plane strain of $\epsilon_1 < 0.1\%$.[27] An atomic-force microscopy (AFM) image of such an AlN(0001) surface is shown in Fig. 1. The surface is characterized by about 30 nm wide terraces and spiral hillocks, similar to GaN surfaces grown under equivalent conditions.[28]

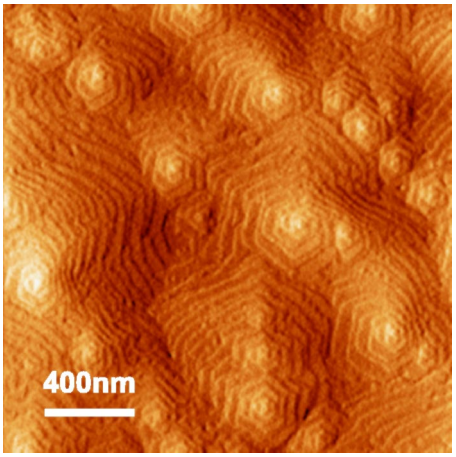

FIG. 1. (Color online) Atomic-force micrograph of an AlN pseudosubstrate.

The growth rate and the GaN coverage have been experimentally determined for each sample by RHEED oscillations occurring during the growth of the wetting layer prior to island formation.[29] Typically, growth rates for different layers (and different samples) were reproducible within about 0.01 monolayers (ML)/s. The GaN coverage was then calculated with a precision better than 0.1 ML. It is worth noting that no measurable influence of the growth rate on GaN island properties has been found in the range between 0.1 and 0.6 ML/s. On the other hand, the Ga/N flux ratio has been found to have a crucial influence on the growth mode,[29] so in this study it was fixed to 0.8 (N-rich conditions). This led to a critical thickness for the SK transition of 2.25 ML.[29,30] The critical thickness was measured for each sample and found to be reproducible within 0.1 ML.

To study the GaN islands *as grown*, the samples were rapidly quenched to room temperature under an *N* flux. *Ex situ* AFM was then used to study the GaN morphology after exposure of the samples to air. The size of surface islands measured by AFM is generally in good agreement with the size found by TEM on AlN-capped samples, indicating that GaN oxidation is insignificant. The island diameters have been corrected for the finite size of the AFM tip (assuming a tip radius of 5 nm). No correction has been applied to island heights.

III. RESULTS

A. Dependence on GaN coverage

The parameter most directly governing the properties of GaN islands grown in the SK mode on AlN is the GaN coverage Θ, which effectively describes the evolution of the islands during growth. To study this evolution, a series of samples was grown at a substrate temperature of 730 °C and a growth rate of 0.15 ML/s. The GaN coverage was varied between 1.8 and 4.6 ML.

Figure 2(a) shows an AFM image of the morphology of GaN layers obtained after the deposition of 1.8 ML, i.e., for a coverage well below the critical thickness of 2.25 ML. We find that the morphology is unchanged with respect to that of the AlN pseudosubstrate: the surface is characterized by about 30 nm wide terraces and spiral hillocks. We can thus infer that the growth of about the first 2 ML of GaN occurs in a layer-by-layer mode since RHEED oscillations are observed.[29]

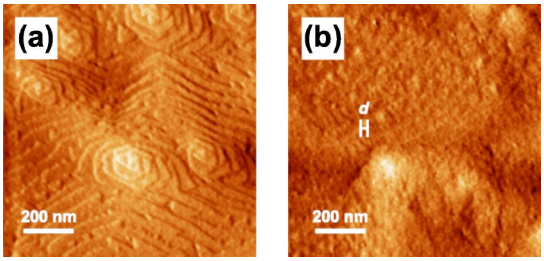

FIG. 2. (Color online) Atomic-force micrograph of the GaN surface morphology for coverages Θ of (a) 1.8 ML and (b) 2.2 ML, respectively. In (b), $d \approx 20$ nm indicates the typical lateral length scale of the 2D precursor islands.

When the second monolayer is completed, the morphology changes, as evidenced in Fig. 2(b) for $\Theta = 2.2$ ML, i.e., immediately before the SK transition. Remainders of terraces and spiral hillocks are still visible, but the surface is characterized on a short scale by 1–2 ML high flat 2D islands with typical diameters of $d \approx 20$ nm [see Fig. 2(b)]. The behavior can thus be described by a transition from a layer-by-layer growth to multilayer growth at around 2.0 ML. Such an occurrence of 2D precursor islands prior to the genuine 2D-3D SK transition has also been observed in the InAs/(Al,Ga) As system.[31–34]

When the growth is continued, the genuine SK transition occurs and 3D GaN islands are formed as shown in Fig. 3. We find that their density increases strongly with GaN coverage and saturates around 3.0 ML at a value of 1.8×10^{11} cm^{-2} [see Figs. 3(a) and 3(b)]. Further GaN deposition does not lead to an increase in island density but instead islands grow in size. However, the islands do not grow continuously in size but a bimodal size distribution is observed [see Figs. 3(c) and 3(d)].

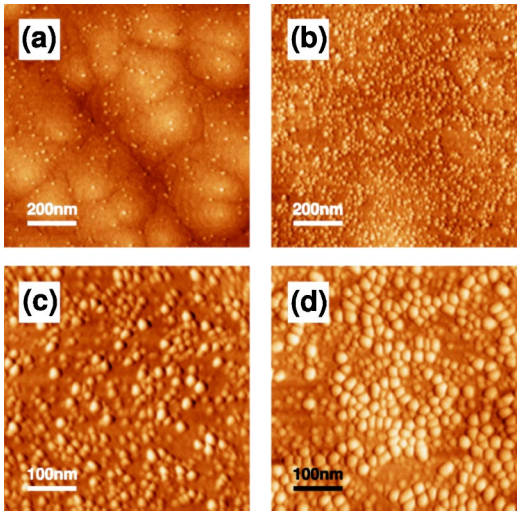

FIG. 3. (Color online) Atomic-force micrograph of GaN surface morphology for coverages Θ of (a) 2.5 ML, (b) 2.8 ML, (c) 3.0 ML, and (d) 4.6 ML, respectively.

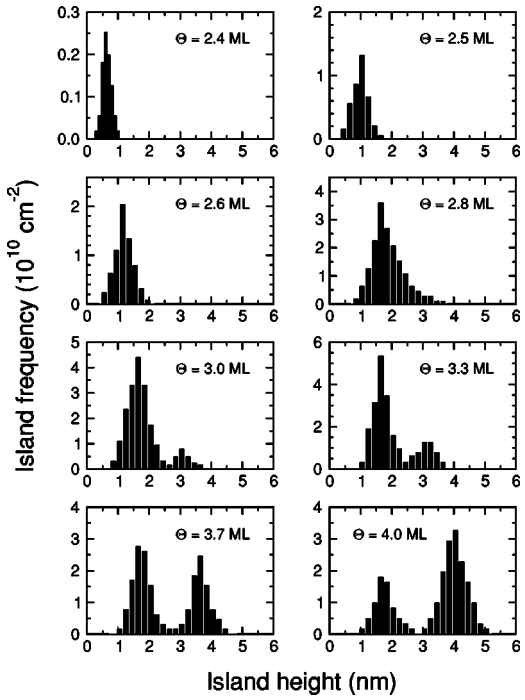

FIG. 4. Height distribution of GaN islands grown on AlN with nominal coverages as indicated. $T_S = 730\,^{\circ}\mathrm{C}$.

The variation of the island height is summarized in Figs. 4 and 5. We see that, initially, the islands' height increases from 0.7 to 1.6 nm between 2.4 and 2.8 ML of GaN coverage. For higher GaN coverage, a bimodal height distribution is observed with the average height of the first mode islands remaining constant at 1.6 nm independent of coverage. In contrast, the average height corresponding to the second mode increases continuously reaching 4.2 nm at 4.7 ML coverage with no sign of saturation in the examined coverage range. Differences in the shapes of mode 1 and mode 2 islands will be discussed below.

The variation of the island density is depicted in Fig. 6. We observe that the total density increases strongly after the SK transition but saturates after 2.8 ML, i.e., at the coverage where the island size distribution becomes bimodal. The partial densities of the two modes are shown in the inset in Fig. 6. For coverages below 2.8 ML, the density of mode 1 islands is identical with the total density and increases strongly with coverage. After the deposition of 2.8 ML, the density of mode 2 islands increases strongly, similarly to the behavior of mode 1 islands after the SK transition, while the density of mode 1 islands decreases. As the total island density remains approximately constant, mode 1 islands transform into mode 2 islands, probably with little or no additional nucleation of new (mode 1) islands.

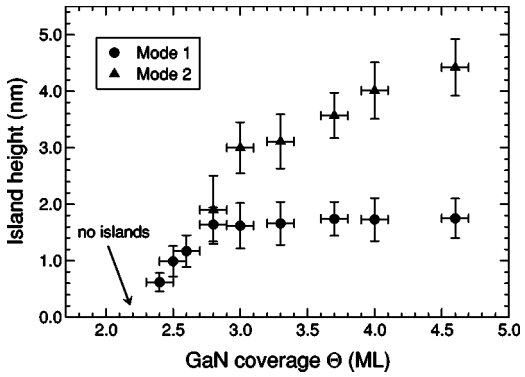

FIG. 5. Average island height as a function of GaN coverage at $T_S = 730\,^{\circ}\mathrm{C}$. Above 2.8 ML a bimodal size distribution is observed.

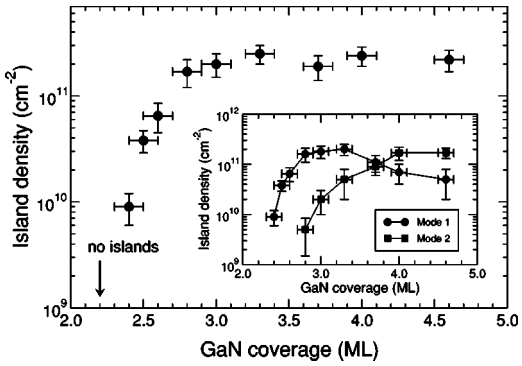

FIG. 6. Total GaN island density as a function of GaN coverage at $T_S = 730\,^{\circ}\mathrm{C}$. The inset shows the partial density of the islands in the two modes. We observe that mode 1 islands transform into mode 2 islands after the deposition of about 2.8–3.0 ML.

B. Dependence on substrate temperature

The influence of the substrate temperature was studied in a series of samples with $\Theta = 3.0$ ML deposited at substrate temperatures between $T_S = 690\,^{\circ}\mathrm{C}$ and $T_S = 760\,^{\circ}\mathrm{C}$. At still lower temperatures, no SK growth is observed and GaN grows in a pseudo-2D mode,[14,29,30] probably due to excessively low adatom mobility.[35] Higher substrate temperatures are prohibited by our experimental apparatus due to indium bonding of the substrates to the substrate holder. All samples in this series were grown at a growth rate of 0.25 ML/s.

AFM images of the morphology of two GaN layers grown at substrate temperatures of $T_S = 700\,^{\circ}\mathrm{C}$ and $T_S = 760\,^{\circ}\mathrm{C}$, respectively, are shown in Fig. 7. We observe that the total island density decreases rapidly with substrate temperature,in keeping with previous results[15] and also with results obtained for the InAs/GaAs (Ref. 36) and Ge/Si (Ref. 37) systems. The variation of the GaN island density as a function of substrate temperature for a coverage of $\Theta = 3.0$ ML is de-

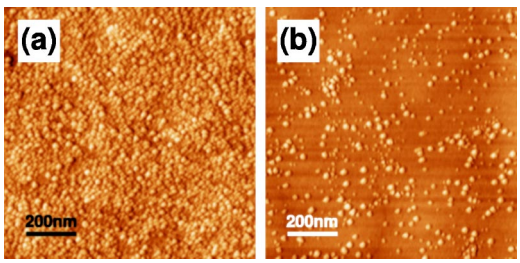

FIG. 7. (Color online) Atomic-force micrograph of GaN surface morphology as a function of substrate temperature: (a) $T_S = 700\,^{\circ}\mathrm{C}$ and (b) $T_S = 760\,^{\circ}\mathrm{C}$.

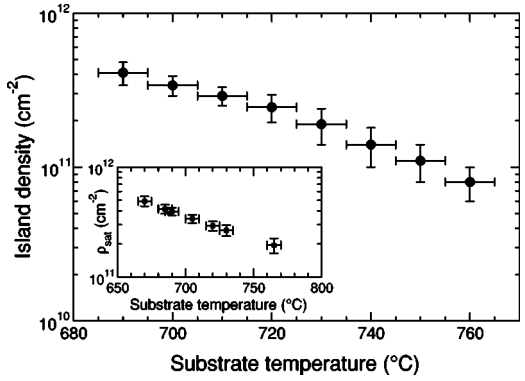

FIG. 8. GaN island density ρ for a coverage of $\Theta = 3.0$ ML as a function of substrate temperature T_S. The inset shows the island saturation density as a function of substrate temperature.

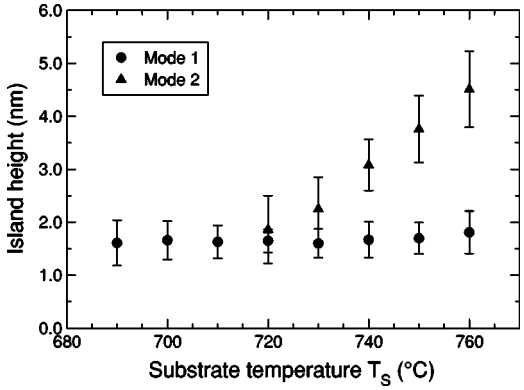

FIG. 10. Average island height as a function of substrate temperature for a GaN coverage of $\Theta = 3.0$ ML. Above 720 °C a bimodal size distribution is observed.

picted in Fig. 8. We find an approximately exponential decrease of the island density with increasing substrate temperature from 4.1×10^{11} cm^{-2} at $T_S = 690$ °C to 8.0×10^{10} cm^{-2} at $T_S = 760$ °C.

As we have seen above, the island density tends to saturate at sufficiently high GaN coverage. This saturation density is shown as a function of substrate temperature in the inset in Fig. 8. For substrate temperatures of $T_S \leqslant 730$ °C, the saturation density is similar to the density for $\Theta = 3.0$ ML, in agreement with the results in the last section. However, for higher substrate temperature, the saturation density is significantly higher, indicating that saturation occurs for GaN coverages larger than 3.0 ML.

Figure 9 shows the island height distribution for $\Theta = 3.0$ ML and substrate temperatures as indicated. The behavior is summarized in Fig. 10. We find a single approximately Gaussian distribution (in the limit of the statistical precision) at a height of 1.6 nm for substrate temperatures $T_S \leqslant 720$ °C. These islands correspond to the mode 1 islands observed at $T_S = 730$ °C as discussed above. At low temperature, the distribution is thus still monomodal after 3.0 ML. For $T_S = 730$ °C, a shoulder appears at the high island side of the distribution and transforms into a clearly separated second mode at higher temperatures. Hence, we find that bimodal distributions occur earlier (for lower GaN coverage) at higher substrate temperature. Another remarkable finding is that the height of the mode 1 islands remains constant as a function of temperature, whereas the height of mode 2 islands increases with temperature, again without signs of saturation in the examined temperature range.

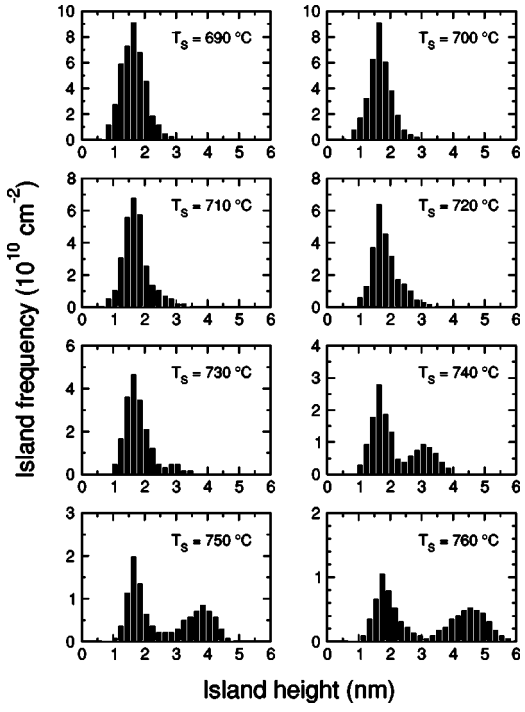

FIG. 9. Height distribution of GaN islands grown on AlN at substrate temperatures as indicated. $\Theta = 3.0$ ML.

IV. DISCUSSION

The above results demonstrate the occurrence of bimodal island size distributions at high GaN coverage and/or substrate temperature; at low GaN coverage and/or substrate temperature, the size distribution is monomodal. Remarkably, when bimodal distributions occur, the size of mode 1 islands (smaller islands) appears independent of growth parameters such as GaN coverage and substrate temperature.

As discussed above, the variation of partial densities of both modes implies that, initially, mode 1 islands are nucleated, their density saturates and the growth mainly proceeds further by transformation of mode 1 islands into mode 2 islands. Thus the question arises, whether this transformation involves a shape change of the islands similar to the behavior observed in the Ge/Si system, where pyramidal islands were observed to transform into "dome-shaped" islands during growth.[21,38] Some information about the island shape can be gathered by RHEED. The RHEED images corresponding to pure mode 1 island morphologies and morphologies with a mixture of mode 1 and mode 2 islands (but with a majority of mode 2 islands) are both characterized by the same $\{10\bar{1}3\}$ facets, showing a sixfold rotation symmetry. It thus appears that both types of islands are (truncated) hexagonal pyramids with $\{10\bar{1}3\}$ sidewalls, in agreement with previous results.[14,15] However, it is clear that the shape of such islands

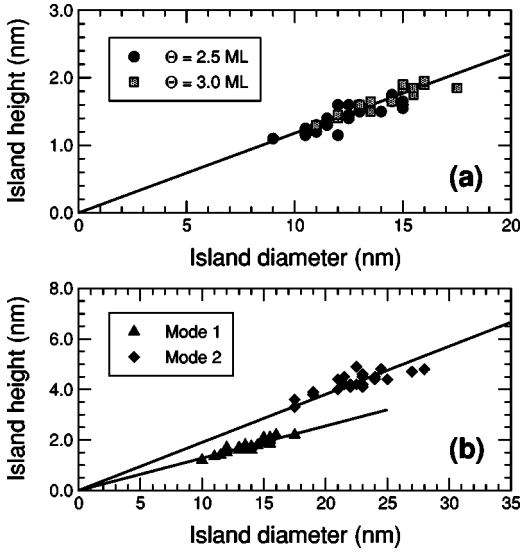

FIG. 11. (a) Island height as a function of diameter for mode 1 islands obtained for two GaN coverages, as indicated. $T_S=730°C$. The solid line corresponds to an aspect ratio of $\tau=0.12$. (b) Island height as a function of diameter for mode 1 and mode 2 islands. $T_S=730°C$, $\Theta=4.0$ ML. The solid lines correspond to aspect ratios of $\tau=0.13$ for mode 1 and $\tau=0.19$ for mode 2, respectively.

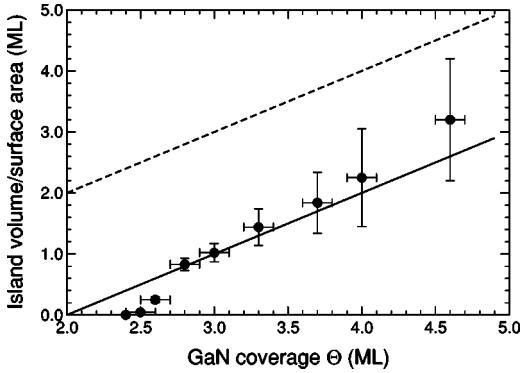

FIG. 12. Total volume per surface area contained in 3D GaN islands as a function of coverage. The solid line indicates the expected behavior for a constant 2 ML thick wetting layer, whereas the dashed line indicates the expected behavior for no wetting layer at all.

cannot be obtained from the RHEED pattern alone and further work is necessary to determine the precise shape of both types of islands.

A more detailed analysis can be done by extracting the aspect ratio τ of the islands from the AFM data. Figure 11(a) depicts the aspect ratio of mode 1 islands for two different GaN coverages (at which monomodal height distributions are observed) at a substrate temperature of 730 °C. In spite of the absolute increase of the islands' size, their aspect ratio remains constant and we find $\tau=0.12$. As shown in Fig. 11(b), the aspect ratio of mode 1 islands remains constant ($\tau=0.13$) after the transition to a bimodal distribution but the mode 2 islands have a significantly larger aspect ratio of $\tau=0.19$. Both aspect ratios correspond to truncated pyramids[39] but mode 1 islands are flatter.

From the aspect ratio data, we can further calculate the amount of GaN contained in the 3D islands as a function of deposited GaN. The result is shown in Fig. 12. We find that the data are consistent with a 2 ML thick wetting layer, independent of the amount of deposited GaN. It thus appears that the wetting layer is stable and does not (or only very weakly) contribute to island growth in this system. The deviation for GaN coverages just after the critical thickness of 2.25 ML can be explained by the presence of 2D precursor islands, which still contain significant material but are not taken into account as 3D islands. The precursor islands become unstable after the SK transition, decay, and contribute to 3D island growth.

A. Equilibrium model

The occurrence of bimodal island size distributions suggests that the total island energy as a function of island size has minima corresponding to mode 1 and mode 2 islands, which are separated by an energetic barrier. From a standpoint of growth kinetics, this barrier has to be overcome if a mode 1 island wants to increase its size. Also, elastic island-island interactions will tend to decrease the island density, which will favor larger islands at higher coverage.

The observation that the size of mode 2 islands increases with coverage without a sign of saturation raises the question if an energy minimum actually exists for these islands. Ripening has been observed in the GaN/AlN system (although not under N-rich conditions),[15] and an alternative hypothesis would be for the configurations to lie along an unstable Ostwald ripening trajectory. In order to understand more precisely why the observed bimodal island distributions form, it is desirable to employ a model to analyze the island size distributions and other features of the growth process.

Only a very limited number of models are available in the literature to make definite predictions about island distributions under specific growth conditions. One such model has been developed to describe bimodal island distributions in the Ge/Si system using an equilibrium statistical mechanics formalism based on island elastic energetics. Previously, this model has only been applied to the Ge/Si system.[26] In the nitride system, Nakajima *et al.*[40] have theoretically derived thickness-composition phase diagrams for the expected growth mode for GaInN/GaN and GaInN/AlN, using known materials parameters. However they did not take into account the shapes and sizes of experimentally observed nitride nanostructures, nor did they seek to calculate size distributions. The approach we take here is to fit the equilibrium model to the AFM data on nitride nanostructure size distributions. The goal is an assessment of whether the bimodal distributions of nanostructures are consistent with thermodynamic equilibrium or if they rather correspond to kinetically limited ripening trajectories. At present, we have focused on the coverage dependence. We find that it is possible to fit the equilibrium model reasonably well to the experimental distributions, suggesting that GaN/AlN growth may actually proceed close to equilibrium.

The thermodynamic equilibrium model makes explicit predictions for the form of bimodal epitaxial nanostructure distributions,[26] based on the island elastic energetics at a

given value of the chemical potential. The island elastic energy is of the form introduced by Shchukin *et al.*,[19] where the internal energy ϵ_i of the ith individual island of type X and volume ν_i is as follows:

$$\epsilon_i = A_X \nu_i + B_X \nu_i^{2/3} + C_X \nu_i^{1/3} + D_X. \quad (1)$$

The elastic energetics depend on the size and shape of the nanostructures, including the bulk elastic relaxation (first term) and the surface (second term) and edge energies, as well as a mean field description of the elastic energy associated with the interactions between nanostructures (also in the second term). Note that for convenience in fitting we have expanded the edge relaxation energy, $\nu^{1/3}\ln(a/\nu^{1/3})$, about the peak volume, giving rise to the last two terms in the energy.[21]

The island size distribution $f(\nu_i)$ depends on this ϵ_i through[26]

$$f(\nu_i) = \exp\left(-\frac{\epsilon_i - \mu\nu_i}{k_B T_S}\right), \quad (2)$$

where μ is the chemical potential per atomic volume and k_B is the Boltzmann constant. Unlike in the most recent developments of the equilibrium model,[26] we have not, as yet, undertaken a self-consistent calculation of the chemical potential. Instead, we have taken a similar approach to Williams *et al.*[21] Using the expressions for the distributions (2) and internal energies (1), we have fitted the model parameters A, B, C, D, and μ, to the available data at all coverages in order to determine how the various contributions to the elastic energy change as a function of growth conditions.

We then used our empirical functions to fit the model across multiple data sets, to determine how well the optimized model compares with the overall behavior of the system. Unfortunately, experimental data on the values of the surface and edge parameters in the GaN/AlN system are not available. The fit values we have determined are constrained only by general considerations:[26] B is taken to be dependent on the coverage due to the island interactions, μ is taken to be a nonlinear function of coverage and temperature due to its dependence on the chemical potential, and the parameters A, C, and D are constant. Based on the results of the Ge/Si model, we expect B to vary linearly with coverage over the range of interest 1 ML $<\Theta<$ 5 ML: $B(\Theta)=B_0+b\Theta$.

The parameters were fit to the experimental data at $T_S = 730\,^\circ$C, producing the following best fit: $\Delta A \equiv A_L - A_S = 0.00110$, $B_{S0} = -0.200$, $b_S = 0.225$, $C_S = -5.35$, $D_S = 9.34$, $B_{L0} = -0.660$, $b_L = 0.223$, $C_L = -5.55$, and $D_L = 21.7$. The units for these parameters are such that energy is measured in $k_B T_S$ with $T_S = 730\,^\circ C$, ν is measured in nm^3 and Θ is measured in ML. Given these parameters, $\mu(\Theta)$ is related to the coverage through the volume sum rule [Eq. (9) of Ref. 26]. The island size distributions resulting from the fit at $\Theta = 3.0$ and 3.7 ML are shown in Fig. 13. The fit parameters appear to be consistent with the known properties of the GaN/AlN system—for example, the B parameter, relating to the surface energy of the islands shows a similar variation for each island type, which is unsurprising if both island types are dominated by the same facet.

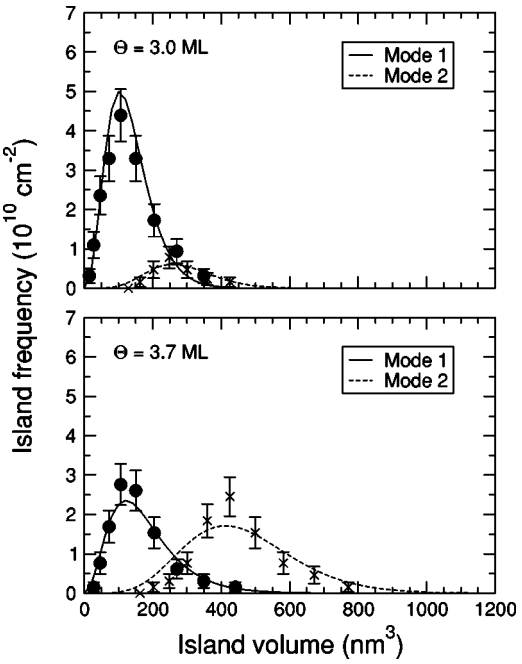

FIG. 13. Comparison of experimentally observed island size distributions (see Fig. 4) at 730 °C with fitted island size distributions for both the smaller (circles) and larger (crosses) islands, for coverages of 3.0 and 3.7 ML, as indicated.

The results of the fit are good, with a total figure of merit of $Q = 0.22$ across the entire set of data presented in Fig. 4. Typically a Q value this high would indicate an extremely good fit. However, the limited number of counts in the peaks prevents us from making very strong claims that the model is thoroughly validated for the GaN/AlN system. For comparison we have also attempted to fit the data with two other functional forms: the model of Williams *et al.*,[21] and the heuristic sum of two Gaussian distributions. These fits were markedly worse, and it was not possible to find parameters that fit the entire set of data with a reasonable Q value. It would also be informative to attempt to fit these data to a kinetic model, but no predictive ripening model is yet available in the literature. From these findings we may infer that the fit to the equilibrium model is consistent with the experimental distributions but larger data sets and/or tighter physical constraints on the parameters are required in order to make a definitive statement about the validity of the model in describing the GaN/AlN system.

V. CONCLUSION

Using *ex situ* AFM, we have studied the evolution of thin GaN layers grown by plasma-assisted MBE on AlN(0001) at substrate temperatures between 700 and 750 °C. Initially, 2 ML of GaN grow in a 2D mode, followed by the occurrence of 2D islands. These islands act as precursors for 3D islands, which appear after an SK transition around 2.3 ML. During further growth, in particular at higher temperatures, a bimodal island size distribution is observed. Remarkably, the size of mode 1 islands is found to be independent of coverage and temperature, whereas the size of mode 2 islands

increases with coverage and temperature. The analysis of the partial island densities reveals that, while the total island density remains constant, mode 1 islands transform during growth into mode 2 islands. The aspect ratio of the islands is measured for both types of islands and it is found that they are characterized by distinctively different aspect ratios, although no additional or different facets appear in the RHEED pattern due to mode 2 islands.

The coverage dependence of the island height distributions at a substrate temperature of 730 °C is fitted to an equilibrium model for SK growth. We find satisfactory agreement with the experimental data, suggesting that GaN growth may actually proceed close to equilibrium at this growth temperature and that the islands may not be subject to Ostwald ripening. As more data become available, this fitting procedure could be extended to fully test the validity of the model. Further experiments on the annealing of dot arrays at growth temperature might also contribute to clarify to what extent the growth proceeds near equilibrium or if kinetic effects are predominant.

ACKNOWLEDGMENTS

The authors would like to thank O. Briot (Université Montpellier II, France) for providing the GaN templates and H. Mariette (Université Joseph Fourier, Grenoble, France) for many stimulating discussions. R.E.R.'s contribution to this work was performed under the auspices of the U.S. Department of Energy by the University of California, Lawrence Livermore National Laboratory, under Contract No. W-7405-Eng-48.

*Present address: Department of Chemical Engineering and Materials Science, University of Minnesota, Minneapolis, Minnesota 55455-0132, USA.

†Present address: Department of Materials Science and Metallurgy, University of Cambridge, Pembroke Street. Cambridge CB2 3QZ, United Kingdom.

[1] Y. Arakawa and H. Sakaki, Appl. Phys. Lett. **40**, 939 (1982).

[2] D. Bimberg, N. Kristaedter, N. N. Ledentsov, Z. I. Alferov, P. S. Kop'ev, and V. M. Ustinov, IEEE J. Sel. Top. Quantum Electron. **3**, 196 (1997).

[3] A. A. Odintsov, Appl. Phys. Lett. **58**, 2695 (1991).

[4] L. P. Kouwenhoven, A. T. Johnson, N. C. van der Vaart, C. J. P. M. Harmans, and C. T. Foxon, Phys. Rev. Lett. **67**, 1626 (1991).

[5] D. Loss and D. P. DiVincenzo, Phys. Rev. A **57**, 120 (1998).

[6] M. Bayer, P. Hawrylak, K. Hinzer, S. Fafard, M. Korkusinski, Z. R. Wasilewski, O. Stern, and A. Forchel, Science **291**, 451 (2001).

[7] For reviews see, e.g., W. Seifert, N. Carlsson, M. Miller, M. E. Pistol, L. Samuelson, and L. R. Wallenberg, Prog. Cryst. Growth Charact. Mater. **33**, 423 (1996); D. Bimberg, M. Grundmann, and N. N. Ledentsov, *Quantum Dot Heterostructures* (Wiley, Chichester, 1999).

[8] L. Goldstein, F. Glas, J. Y. Marzin, M. N. Charasse, and G. Le Roux, Appl. Phys. Lett. **47**, 1099 (1985).

[9] D. Leonard, M. Krishnamurthy, C. M. Reaves, S. P. DenBaars, and P. M. Petroff, Appl. Phys. Lett. **63**, 3203 (1993).

[10] J. M. Moison, F. Houzay, F. Barthe, L. Leprince, E. André, and O. Vatel, Appl. Phys. Lett. **64**, 196 (1994).

[11] D. J. Eaglesham and M. Cerullo, Phys. Rev. Lett. **64**, 1943 (1990).

[12] Y.-W. Mo, D. E. Savage, B. S. Swartzentruber, and M. G. Lagally, Phys. Rev. Lett. **65**, 1020 (1990).

[13] S. H. Xin, P. D. Wang, A. Yin, C. Kim, M. Dobrowolska, J. L. Merz, and J. K. Furdyna, Appl. Phys. Lett. **69**, 3884 (1996).

[14] B. Daudin, F. Widmann, G. Feuillet, Y. Samson, M. Arlery, and J.-L. Rouvière, Phys. Rev. B **56**, R7069 (1997).

[15] F. Widmann, B. Daudin, G. Feuillet, Y. Samson, J.-L. Rouvière, and N. T. Pelekanos, J. Appl. Phys. **83**, 7618 (1998).

[16] B. Damilano, N. Grandjean, F. Semond, J. Massies, and M. Leroux, Appl. Phys. Lett. **75**, 962 (1999).

[17] C. Adelmann, N. Gogneau, E. Sarigiannidou, J.-L. Rouvière, and B. Daudin, Appl. Phys. Lett. **81**, 3064 (2002); N. Gogneau, D. Jalabert, E. Monroy, T. Shibata, M. Tanaka, and B. Daudin, J. Appl. Phys. **94**, 2254 (2003).

[18] J. Brown, F. Wu, P. M. Petroff, and J. S. Speck, Appl. Phys. Lett. **84**, 690 (2004).

[19] V. A. Shchukin, N. N. Ledentsov, P. S. Kop'ev, and D. Bimberg, Phys. Rev. Lett. **75**, 2968 (1995); V. A. Shchukin and D. Bimberg, Rev. Mod. Phys. **71**, 1125 (1999).

[20] I. Daruka and A.-L. Barabási, Phys. Rev. Lett. **79**, 3708 (1997); Appl. Phys. Lett. **72**, 2102 (1999).

[21] R. S. Williams, G. Medeiros-Ribeiro, T. I. Kamins, and D. A. A. Ohlberg, Annu. Rev. Phys. Chem. **51**, 527 (2000).

[22] C. Priester and M. Lannoo, Phys. Rev. Lett. **75**, 93 (1995).

[23] Y. Chen and J. Washburn, Phys. Rev. Lett. **77**, 4046 (1996).

[24] D. E. Jesson, G. Chen, K. M. Chen, and S. J. Pennycook, Phys. Rev. Lett. **80**, 5156 (1998).

[25] F. M. Ross, J. Tersoff, and R. M. Tromp, Phys. Rev. Lett. **80**, 984 (1998).

[26] R. E. Rudd, G. A. D. Briggs, A. P. Sutton, G. Medeiros-Ribeiro, and R. S. Williams, Phys. Rev. Lett. **90**, 146101 (2003).

[27] E. Bellet-Amalric, C. Adelmann, E. Sarigiannidou, J.-L. Rouvière, G. Feuillet, E. Monroy, and B. Daudin, J. Appl. Phys. **95**, 1127 (2004).

[28] C. Adelmann, J. Brault, D. Jalabert, P. Gentile, H. Mariette, G. Mula, and B. Daudin, J. Appl. Phys. **91**, 9638 (2002).

[29] G. Mula, C. Adelmann, S. Moehl, J. Oullier, and B. Daudin, Phys. Rev. B **64**, 195406 (2001).

[30] C. Adelmann, Ph.D. thesis, Université Joseph Fourier, Grenoble, 2002.

[31] G. E. Cirlin, G. M. Guryanov, A. O. Golubok, S. Y. Tipissev, N. N. Ledentsov, P. S. Kop'ev, M. Grundmann, and D. Bimberg, Appl. Phys. Lett. **67**, 97 (1995).

[32] H. Kitabayashi and T. Waho, J. Cryst. Growth **150**, 152 (1995).

[33] T. R. Ramachandran, R. Heitz, P. Chen, and A. Madhukar, Appl. Phys. Lett. **70**, 640 (1997).

[34] P. Ballet, J. B. Smathers, and G. J. Salamo, Appl. Phys. Lett. **75**, 337 (1999); P. Ballet, J. B. Smathers, H. Yang, C. L. Workman,

and G. J. Salamo, J. Appl. Phys. **90**, 481 (2001).
[35] T. Zywietz, J. Neugebauer, and M. Scheffler, Appl. Phys. Lett. **73**, 487 (1998).
[36] R. Leon, T. J. Senden, Y. Kim, C. Jagadish, and A. Clark, Phys. Rev. Lett. **78**, 4942 (1997).
[37] T. I. Kamins, E. C. Carr, R. S. Williams, and S. J. Rosner, J. Appl. Phys. **81**, 211 (1997).
[38] G. Medeiros-Ribeiro, A. M. Bratkovski, T. I. Kamins, D. A. A. Ohlberg, and R. S. Williams, Science **279**, 353 (1998).
[39] The aspect ratio for a full pyramid with $\{10\bar{1}3\}$ facets is $\tau = 0.29$.
[40] K. Nakajima, T. Ujihara, S. Miyashita, and G. Sazaki, J. Appl. Phys. **89**, 146 (2001).